Electron–vibration coupling in time-dependent density-functional theory: Application to benzene

G. F. Bertsch, A. Schnell, and K. Yabana

Citation: J. Chem. Phys. **115**, 4051 (2001); doi: 10.1063/1.1390513
View online: http://dx.doi.org/10.1063/1.1390513
View Table of Contents: http://jcp.aip.org/resource/1/JCPSA6/v115/i9
Published by the American Institute of Physics.

Additional information on J. Chem. Phys.

Journal Homepage: http://jcp.aip.org/
Journal Information: http://jcp.aip.org/about/about_the_journal
Top downloads: http://jcp.aip.org/features/most_downloaded
Information for Authors: http://jcp.aip.org/authors

ADVERTISEMENT

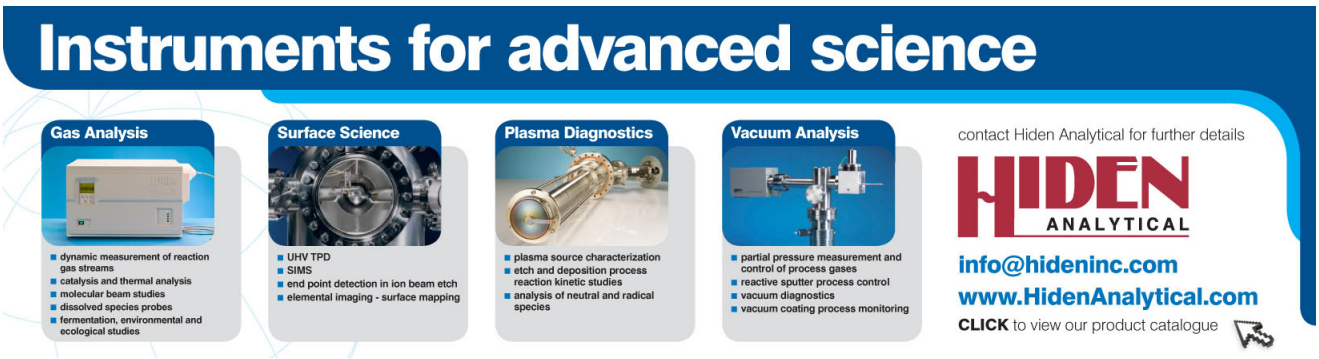

Downloaded 21 Mar 2013 to 69.91.142.29. Redistribution subject to AIP license or copyright; see http://jcp.aip.org/about/rights_and_permissions

Electron–vibration coupling in time-dependent density-functional theory: Application to benzene

G. F. Bertsch[a] and A. Schnell
Institute for Nuclear Theory, University of Washington, Seattle, Washington 98125

K. Yabana
Institute of Physics, University of Tsukuba, Tsukuba 305-8571, Japan

(Received 27 November 2000; accepted 19 June 2001)

As a test of the time-dependent density-functional theory (TDDFT) for electron–vibration coupling, we apply it to the optical properties of the π–π^* transitions in benzene. Quantities calculated are the envelopes of the Franck–Condon factors of the electronic transitions and the oscillator strengths of symmetry-forbidden transitions. The strengths of the π–π^* transitions span three orders of magnitude and are reproduced to better than 35% by the theory. Comparable agreement is found for the Franck–Condon widths. We conclude that rather detailed information about the effects of the electron–vibrational coupling can be obtained with the TDDFT. © *2001 American Institute of Physics.* [DOI: 10.1063/1.1390513]

I. INTRODUCTION

The time-dependent density-functional theory (TDDFT) is now being widely applied in both chemistry and condensed matter physics to describe electron excitations, the dielectric function, and the optical absorption strength function. (For reviews, see Refs. 1 and 2. More recent citations can be found in Ref. 3.) While not as accurate for excitations as the ordinary DFT is for ground properties, the theory has considerable predictive power and is computationally quite tractable, allowing calculations for large molecules. These applications have been for purely electronic excitations. The DFT is also very successful in describing vibrational properties (e.g., see Ref. 4 and cited references for the frequencies and transitions transition strengths of the infrared active vibrations in C_{60}). In view of the success in both these areas, it is interesting to apply the TDDFT in more general context, allowing the nuclear degrees of freedom to interact with the electronic excitations.

In this work, we have chosen the benzene model for an exploratory study of the electron–vibration coupling. Benzene is an excellent example for this purpose because its spectrum has been very well characterized, both the electronic excitations and the vibrational excitations. The TDDFT has been shown to be quite accurate for calculating the energies of the π–π^* transitions as well as the transition strength of the strong E_{1u} transition at 7 eV. Also, the electron–vibrational coupling has been calculated to rather good accuracy by other methods.[5]

The TDDFT is an approximation to the dynamics that is valid at short times, and we wish to examine the effects of the electron–vibrational coupling that are visible in the short-time response. One effect is the promotion of strength into symmetry-forbidden electronic transitions due to vibration couplings. There are two such transitions in the π–π^* spectrum of benzene, the B_{2u} around 5 eV and the the B_{1u} just above 6 eV. Another effect of the coupling is to spread the transition strength over a spectral region via the Franck–Condon factors for individual vibrational states. At short times, the spreading is describable in terms of moments of the strength functions, and we shall examine the lowest order moments induced by the couplings. We thus can avoid the problem of constructing the vibrational eigenstates on the excited-energy surface, which is nontrivial due to the stronger mixing there.

II. THEORY AND CALCULATIONAL DETAILS

The formal basis of the present calculation is the semiclassical short-time analysis given by Heller.[6] That article presents several approximations for calculating the strength function with inclusion of the effects of the vibrational degree of freedom. The simplest and the one we employ here is the well-known reflection approximation. While less accurate than the others on the average frequency of the absorption profile, it reproduces the width (second moment) very well [for the numerical case presented in Ref. 6, the reflection approximation only has a 2% error in the root-mean-square (rms) width.]. We shall also assume that the vibrations are harmonic in the ground state. In that case, the semiclassical theory gives a Gaussian envelope of the Franck–Condon factors. This can also be derived analytically in a harmonic oscillator model.[7]

To apply the reflection approximation, one first calculates the electronic transition strength function as a function of the vibrational normal mode coordinates Q_k. Both the energy of the electronic excitations E_i and their transition strength f_i dependence on Q_k. In the case of forbidden transitions promoted by vibrations, the transition strength depends quadratically on the coordinate for small displacements and the strength function can be parameterized as

$$f_i(Q_k) = f_{ik} Q_k^2. \tag{1}$$

[a]Electronic mail: bertsch@phys.washington.edu

 © 2001 American Institute of Physics

Downloaded 21 Mar 2013 to 69.91.142.29. Redistribution subject to AIP license or copyright; see http://jcp.aip.org/about/rights_and_permissions

The total transition strength is then given by

$$\overline{f_i} = \sum_k f_{ik} Q_{0k}^2, \tag{2}$$

where Q_{0k} is the rms amplitude of the zero-point motion in the ground vibrational state (at finite temperature the rms amplitude is increased by a factor $1/\sqrt{\tanh(\hbar\omega_k/2k_BT)}$). To get the widths of the states in the reflection approximation, we first expand the excitation energy in a power series in the coordinates

$$E_i(Q_k) = E_i(0) + K_{ik}Q_k + \tfrac{1}{2}K'_{ik}Q_k^2 + \cdots .$$

Then for small K' the profile of the absorption is approximately Gaussian with an rms width given by

$$\sigma_i = \sqrt{\sum_k (K_{ik}Q_{0k})^2}. \tag{3}$$

We return now to the problem of calculating the electronic excitation strength function in the TDDFT. The theory starts with the electronic wave function on the ground potential energy surface (at fixed Q_k). The wave function is obtained by solving the Kohn–Sham equations for the electron orbitals ϕ_i

$$-\frac{\nabla^2}{2m}\phi_i + \frac{\delta \mathscr{E}}{\delta n}\phi_i = \epsilon_i \phi_i .$$

Here $\mathscr{E}$ is the nonkinetic energy functional of the DFT. In this work we use a simple local density approximation (LDA) functional[8] for the electron–electron interaction in $\mathscr{E}$ and a pseudopotential approximation[9,10] to treat the interaction of the valence electrons with the ions. As in our previous work,[11] we solve equations in a coordinate space representation using a mesh. The Hamiltonian operator is sparse in this representation and it also is convenient in checking convergence, which is controlled by the mesh parameters. The important numerical parameters in the calculation are the mesh spacing, taken as $\Delta x = 0.3$ Å, and the volume in which the wave functions are calculated, which we take as a sphere of radius 7 Å. With these parameters, orbital energies are converged to better than 0.05 eV.

The excited states of the TDDFT are calculated in the same representation, using the same Kohn–Sham operator as in the ground-state calculation. In earlier work we solved the equations of TDDFT in real time, which is efficient for calculating the complete optical response. However, in the application here, the excitations of interest are among the lowest 10 eigenmodes of the linearized equations, and it is more efficient to solve the matrix equations directly. The linearized equations are very similar to the random phase approximation (RPA) equations, having a structure

$$-\frac{\nabla^2}{2m}\phi_i^{\pm} + \frac{\delta \mathscr{E}}{\delta n}\phi_i^{\pm} + \frac{\delta^2 \mathscr{E}}{\delta n^2}\delta n\, \phi_i = (\epsilon_i \pm \omega)\phi_i^{\pm} .$$

Here the transition density δn and normalization are given by

$$\delta n = \sum_i \phi_i(\phi_i^+ + \phi_i^-), \quad \langle \phi_i^+ | \phi_i^+ \rangle - \langle \phi_i^- | \phi_i^- \rangle = 1.$$

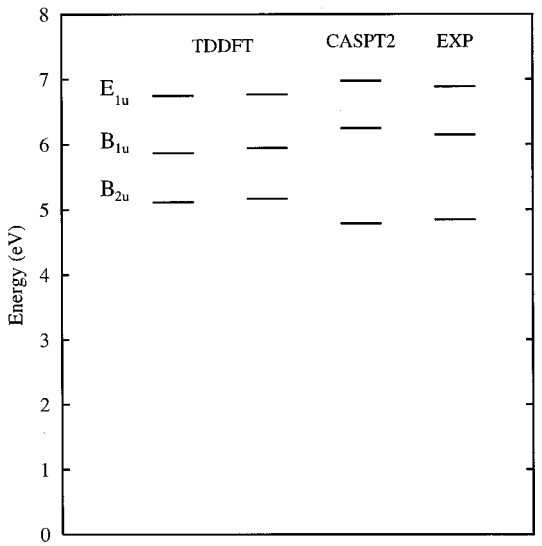

FIG. 1. Electronic excitations in benzene. The two TDDFT calculations our own (leftmost) and one of those of Ref. 3 (next on right). The next level scheme shows the CI calculation of Ref. 20. The rightmost column shows the empirical spectrum as compiled in Ref. 3.

The equations are solved by the conjugate gradient method for the generalized eigenvalue problem.[12]

III. RESULTS

The pure electronic spectra in the π–π^* manifold are shown in Fig. 1, compared with experiment and with other calculations. It is seen that the TDDFT gives an excellent account of the energies. In fact the TDDFT gives a good description of the higher-frequency absorption including σ–σ^* transitions as well.[11] One should also note the close agreement between our TDDFT results calculated with a simple local density approximation and the results of Ref. 3 that used the generalized gradient approximation.

We next discuss the vibrations. The vibrational wave functions are only needed on the ground potential energy surface for the purposes of applying the reflection approximation. We have opted to treat the vibrations phenomenologically, using the empirical force field of Ref. 13, which fits the observed frequencies extremely well. *Ab initio* calculations of the force field in DFT have also reached a high level of accuracy.[14–16] However, as mentioned earlier, our purpose here is to focus on the electron–vibrational coupling, and to that end it is both simpler and more direct to use the empirical force field. We include all the vibrations in our calculations, but we find, in agreement with other work, that the most important vibrations are the A_{1g} for the widths

TABLE I. Properties of selected vibrational modes of benzene, computed with the force field of Ref. 13. Modes are numbered in the Wilson scheme.

	A_{1g}		B_{2g}			E_{2g}		
mode	1	2	4	5	6	7	8	9
$\hbar\omega$ (meV)	123	381	87	122	75	379	198	145
Q_{0k} (Å)	0.13	0.07	0.15	0.13	0.17	0.07	0.10	0.12

Downloaded 21 Mar 2013 to 69.91.142.29. Redistribution subject to AIP license or copyright; see http://jcp.aip.org/about/rights_and_permissions

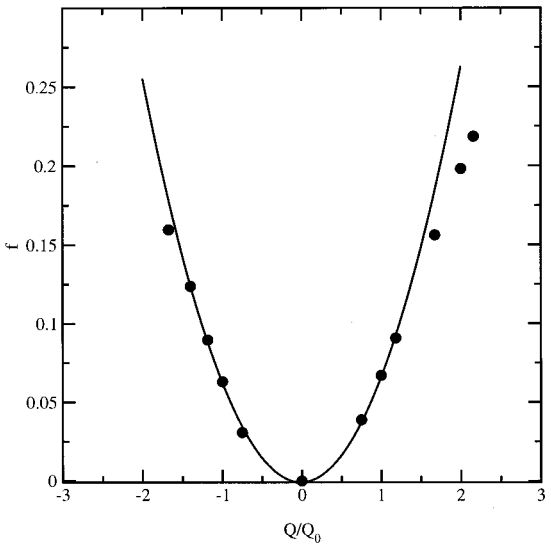

FIG. 2. Dependence of the oscillator strength of the $^1B_{1u}\leftarrow{}^1A_{1g}$ transition on the vibrational coordinate for the 8a mode, and parabolic fit.

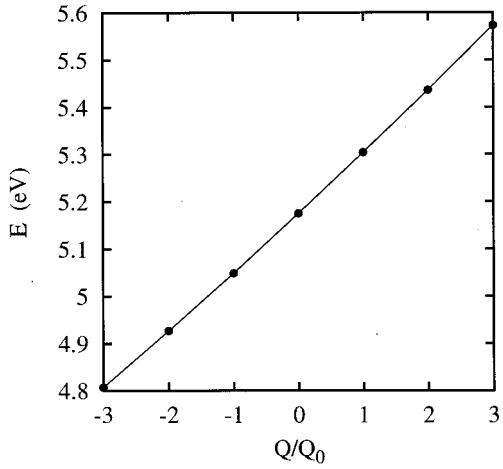

FIG. 3. Dependence of the $^1B_{2u}\leftarrow{}^1A_{1g}$ transition energy on the vibrational coordinate for the mode 1, and linear fit.

and the B_{2g} and E_{2g} modes for the strengths of the forbidden electronic transitions. For reference, we list the properties of these modes in Table I. The displacement of the atoms in the Cartesian basis q_i is related to the normal mode coordinates by $q_i = M_i^{-1/2}\Sigma_k U_{ik} Q_k$ where **U** is an orthogonal matrix and M_i is the mass in daltons of atom i.

In Figs. 2 and 3 we show the vibrational-coordinate dependence of the transition strength f_i and excitation energies E_i in typical cases. We see that the conditions for applying Eqs. (1) and (3) are well satisfied. We may then extract the transition strength f_{ik} and the slope K_{ik} by fitting the Q_k-dependence of these quantities. Inserting in Eqs. (2) and (3), we find the widths and transitions strengths shown in Table II.

Experimentally, the detailed optical properties of the three transitions have been studied gas phase absorption.[17,18] The allowed E_{1u} transition is determined to have a strength in the range $f = 0.9–0.95$. The B_{1u} mode is seen as a shoulder on the E_{1u} peak. Its total transition strength is about a factor of 10 lower than the strong state; Ref. 17 quotes a value $f = 0.09$. The B_{2u} transition is very weak and is seen as a partially resolved set of vibrational transitions with a total strength about $f \approx 1.3\times 10^{-3}$.[17] The strength associated with the most prominent resolved states is 0.6×10^{-3}.[18] We have also assigned widths to the three excitations by a three-term Gaussian fit to the absorption data of Ref. 19.

In the calculation, the only vibrations that contribute in lowest order to the width are the two A_{1g} breathing modes. The vibrations affect all three transitions identically; mode 1 has the larger amplitude of displacement of the carbon atoms and gives the greater contribution. The results agree rather

TABLE II. Vibrational coupling properties in benzene molecule. The upper table shows the predicted rms widths associated with the two A_{1g} vibrations. The total is compared to the CASSCF calculation of Ref. 5 and to experiment (see text). In the middle table, the predicted transition strength associated with the various vibrations are given, with blank entries having values smaller than 10^{-4}. In the lower table, the predicted total transition strength is compared with the CASSCF theory and to experiment (Ref. 17).

Widths (ev)	1	2	Tot.	CASSCF	Expt.
$^1B_{2u}$	0.12	0.03	0.15	0.14	0.18
$^1B_{1u}$	0.12	0.03	0.15	0.14	0.17
$^1E_{1u}$	0.12	0.03	0.15		0.125

$f_{0k}/10^{-3}$	4	5	6	7	8	9	Total
$^1B_{2u}$	⋯	⋯	1.4	0.2	⋯	⋯	1.6
$zz\,^1B_{1u}$	⋯	1.6	0.4	⋯	44	13	59

$\bar{f}/10^{-3}$	TDDFT	CASSCF	Expt.
$^1B_{2u}$	1.6	0.5	1.3
$^1B_{1u}$	59	75	90
$^1E_{1u}$	1100		900–950

Downloaded 21 Mar 2013 to 69.91.142.29. Redistribution subject to AIP license or copyright; see http://jcp.aip.org/about/rights_and_permissions

well with the empirical widths. The magnitude of the widths and its independence of the electronic state can be understood in very simple terms with the Hückel model. This is to be expected, since the excitation energy of the electronic states is mainly due to the orbital energy difference, and that is describe quite well by the Hückel model. For benzene, the energy difference is related to the hopping matrix element β by $E_{\mathrm{LUMO}}-E_{\mathrm{HOMO}}=2\beta$. Allowing changes in the nuclear coordinates, the hopping matrix element will depend on the distance between neighboring atoms d; this may be parameterized by the form

$$\beta(d)=\beta_0\left(\frac{d_0}{d}\right)^{\alpha}.$$

Then the highest occupied molecular orbital–lowest unoccupied molecular orbital (HOMO–LUMO) gap fluctuates due to the breathing mode vibrations with widths given by

$$\Delta E=2\beta_0\alpha\frac{\Delta r}{r},$$

where r is the radial distance of the carbons from the center and Δr is at $Q_k=Q_{0k}$ in an A_{1g} mode. From fitting orbital energies in various conjugated carbon systems one may extract values $\alpha\approx 2.7$ and $\beta_0=2.5\,\mathrm{eV}$.[11] Inserting these values in the above equation, one obtains 0.145 eV for the widths associated with mode 1, quite close to the values obtained by TDDFT. Similar results are obtained for the rms widths of the Franck–Condon factors calculated in the complete active space self-consistent field (CASSCF) theory,[5] which are also reported in the table. One point should also be noted on the comparison with experiment. While the theory gives practically identical widths for all three states, the experimental strength is significantly narrower for the E_{1u} excitation, and this seems to not be understandable in the TDDFT.

Next we examine the transition strengths of the B-transitions induced by the zero-point vibrational motion. In the middle table of Table II we show the contributions by the six active vibrational modes. The main contribution for the B_{2u} transition comes from mode 6. This is also found in the CASSCF theory, and is how the observed spectrum was interpreted in Ref. 18. In the case of the B_{1u} excitation, the TDDFT predicts that the coupling of mode 8 is dominant. Experimentally, the situation is unclear because the vibrational spectrum of the excited state is strongly perturbed. Reference 18 assigns both mode 6 and mode 8 vibrational involvement. Irrespective of the spectral details of the vibrational modes in the excited state, the total transition strength in the reflection approximation is given by the same integral over the ground-state vibrational wave function. As in the case of the widths, the induced B_{1u} transition strength can be understood roughly with the tight-binding model. The charge densities are displaced in the vibration, giving the B_{1u} configuration an induced dipole moment just from the atomic geometry. The Hückel Hamiltonian of the orbital energy is also affected by the changed separations between carbons, and that cause a violation of the B_{1u} symmetry. Finally, the Coulomb interaction, which is mainly responsible for the splitting of the three electronic states, is affected by the changed separations. Of these three mechanisms, only the effect of the symmetry-violation in the Hückel Hamiltonian is important, and mode 8 carries the largest fluctuation in d. Taking the same d-dependence as before, the strength obtained in the tight-binding model is 0.05, rather close to the TDDFT result. The tight-binding model cannot be used to estimate the very weak B_{2u} transition because the charge density on the atomic centers is identically zero.

The lower table gives the empirical transition strengths and comparison to theory. The agreement between theory and experiment is quite good for all states. For the weakest transition, the B_{1u}, the TDDFT gives a transition strength 25% higher than the empirical For the case of the B_{1u} transition, the TDDFT prediction is within 35% of the measured value. We also show the previously reported value for the E_{1u} which is within 20%. We consider this remarkable success of the TDDFT considering that the strengths range over three orders of magnitude.

IV. CONCLUSION

In conclusion, we have shown that the TDDFT gives a semiquantitative account of the effect of zero-point vibrational motion on the optical absorption spectrum in benzene. In this respect this extends the possible domain of utility from the region of infrared absorption, where it is known that the TDDFT gives a description of transition strengths accurate to a factor of 2 or so.[4] We are encouraged by these results to consider the TDDFT for other problems involving the electron–vibrational coupling, such as temperature effects on the optical absorption.

ACKNOWLEDGMENTS

The authors acknowledge stimulating discussions with G. Roepke. The authors also thank J. Giansiracusa for numerical assistance. This work was supported by the Department of Energy under Grant No. DE-FG06-90ER40561.

[1] E. K. U. Gross *et al.*, in *Density Functional Theory II*, edited by R. F. Nalewajski (Springer, Heidelberg, 1996), Vol. 181, p. 81.
[2] M. E. Casida, in *Recent Developments and Applications of Modern Density Functional Theory*, edited by J. M. Seminario (Elsevier, Amsterdam, 1996), Vol. 4, p. 391.
[3] H. Heinze, A. Goerling, and N. Roesch, J. Chem. Phys. **113**, 2088 (2000).
[4] G. F. Bertsch, A. Smith, and K. Yabana, Phys. Rev. B **52**, 7876 (1995).
[5] A. Bernhardsson *et al.*, Chem. Phys. **112**, 2798 (2000).
[6] E. Heller, J. Chem. Phys. **68**, 2066 (1978).
[7] Y. Wang, C. Lewenkopf, D. Tomanek, and G. F. Bertsch, Chem. Phys. Lett. **205**, 521 (1993).
[8] J. Perdew and A. Zunger, Phys. Rev. B **23**, 5048 (1981).
[9] N. Troullier and J. L. Martins, Phys. Rev. B **43**, 1993 (1991).
[10] L. Kleinman and D. Bylander, Phys. Rev. Lett. **48**, 1425 (1982).
[11] K. Yabana and G. F. Bertsch, Int. J. Quantum Chem. **75**, 55 (1999).
[12] W. W. Bradbury and R. Fletcher, Numer. Math. **9**, 259 (1966).
[13] L. Goodman, A. G. Ozkabak, and S. N. Thakur, J. Phys. Chem. **95**, 9044 (1991).
[14] A. Miani, E. Cané, P. Palmieri, A. Trombetti, and N. C. Handy, J. Chem. Phys. **112**, 248 (2000).
[15] J. M. L. Martin, P. R. Taylor, and T. J. Lee, Chem. Phys. Lett. **275**, 414 (1997), and Refs. therein.
[16] E. Albertazzi and F. Zerbetto, Chemical Physics **164**, 92 (1992).
[17] E. Pantos, J. Philis, and A Bolovinos, J. Mol. Spectrosc. **72**, 36 (1978).
[18] A. Hiraya and K. Shobatake, J. Chem. Phys. **94**, 7700 (1991).
[19] H.-H. Perkampus, *UV Atlas of Organic Compounds, Vol. 1* (Butterworth, Verlag Chemie, 1968).
[20] J. Lorentzon, P. Malmquist, M. Fülscher, and B. O. Roos, Theor. Chim. Acta **91**, 91 (1995).

Downloaded 21 Mar 2013 to 69.91.142.29. Redistribution subject to AIP license or copyright; see http://jcp.aip.org/about/rights_and_permissions